Available online at www.sciencedirect.com
ScienceDirect
Nuclear Instruments and Methods in Physics Research B 266 (2008) 3247–3256
NIM B
Beam Interactions with Materials & Atoms
www.elsevier.com/locate/nimb

Study of substrate topographical effects on epithelial cell behavior using etched alpha-particle tracks on PADC films

C.K.M. Ng [a], W.L. Poon [b], W.Y. Li [a], T. Cheung [a], S.H. Cheng [b], K.N. Yu [a,*]

[a] Department of Physics and Materials Science, City University of Hong Kong, Tat Chee Avenue, Kowloon Tong, Kowloon, Hong Kong
[b] Department of Biology and Chemistry, City University of Hong Kong, Tat Chee Avenue, Kowloon Tong, Kowloon, Hong Kong

Received 6 March 2008; received in revised form 5 April 2008
Available online 14 April 2008

Abstract

Micrometer-size pits on the surface of a polymer (polyallyldiglycol carbonate or PADC) substrate created by alpha-particle irradiation and subsequent chemical etching were used to study the topographical effects alone on cell behavior. Vinculin, the cell adhesion and membrane protrusion protein, was used as an indicator of cytoskeletonal reorganization on the substrate and localization of vinculin was used to demonstrate the presence of focal adhesions. In our experiments, vinculin expressed in epithelial HeLa cells cultured on PADC films with track-etch pits, but not in cells cultured on the raw or chemically etched blank films. In other words, vinculin expression was induced by the topography of track-etch pits, while etching of the substrate alone (without alpha-particle irradiation) did not cause up-regulation of vinculin protein expression. HeLa cells cultured on PADC films with track-etch pits also showed changes in cell proliferation, cell area and cell circularity, and were largely contained by the pits. In other words, the cell membrane edges tended to be in contact with the pits. By comparing the correlation between the positions of HeLa cells and the pits, and that between the positions of cells and computer-simulated pits, the tendency for membrane edges of HeLa cells to be in contact with the pits was recognized. This could be explained by inhibition of membrane protrusion at the pits. In conclusion, substrate track-etch pits were an important determinant of epithelial cell behaviors.

PACS: 29.40.Gx; 29.40.Wk; 87.50.−a; 87.50.Gi; 87.52.Ln

Keywords: Alpha-particle irradiation; PADC; HeLa cell; Topography; Vinculin

1. Introduction

Many implant applications involve porous materials. It is now well established that pores introduce topographies onto the substrates, while substrate topographies will control the nature and degree of cell–cell and cell-matrix interactions and determine the morphology and functional induction of cultured cells *in vivo* [1–9]. As a result, a considerable body of research has been devoted to studying the effects of micropores or micropits on cell interactions [10–19]. In particular, the effects of micropores on epithelial tissues have been extensively examined both *in vitro* and *in vivo*. The *in vivo* study by Squier and Collins [20] involved the implantation of Millipore™ filters in pig backskin, which showed the support of tissue growth on filters with pore size of 0.025–1.2 μm, and prevention of downgrowth on filters with larger pore size of 3–8 μm. Similarly, Takeuchi [21] found that migration of chick corneal epithelium was supported on Millipore™ filters with pore size of 0.3–0.45 μm and inhibited on filters with pore size of and larger than 0.8 μm. In a series of systematic studies related to corneal onlay, where the onlay lenticule should be porous to provide nutritional flux between the overlying epithelial tissue and the corneal stroma, the dependence of epithelialization, migration and adhesion of corneal epithelial tissues and/or cells on the presence, size and density of polymeric substrate micropores were identified [22–26].

* Corresponding author. Tel.: +852 27887812; fax: +852 27887830.
E-mail address: peter.yu@cityu.edu.hk (K.N. Yu).

0168-583X/$ - see front matter © 2008 Elsevier B.V. All rights reserved.
doi:10.1016/j.nimb.2008.04.002

However, as commented by Dalton et al. [23], the pores on track-etched membranes introduced both topography and porosity, so it would be impossible to separate the relative contribution of topography and porosity from these pores to the effects on epithelial cells and tissues. By blind-ending the pores to produce 10-μm deep cylindrical pits [25], the increase in tissue migration was found to be independent of fluid flux through the pores and so appeared to occur as a result of surface topography.

Such blind-ended pores bear a resemblance to track-etch pits commonly encountered in ion-irradiated and chemically etched solid-state nuclear track detectors (SSNTDs) [27]. Therefore, an interesting research would be to determine the topographical effects of these track-etch pits on epithelial cell behavior through using the human epithelial HeLa cell line.

It has been established that surface topography affects cell adhesion [23,28,29]. An important cell adhesion structure is the focal adhesions that are specialized regions of the cell membrane and are separated from the substratum by 10–15 nm. Bundles of actin filaments terminate at the focal adhesions where they attach to intergrins through binding proteins [30]. Integrins comprise cell-surface matrix receptors with an extracellular domain that binds to a protein component of the extracellular matrix (ECM) and an intracellular domain that indirectly binds to actin filaments via a complex of attachment proteins, including vinculin [31–33]. Localization of vinculin by immunofluorescence microscopy is therefore often used to demonstrate the presence of focal adhesions [34–36]. Previous studies also showed that substrate microtopography could change the establishment of focal adhesion complexes [37] and could invoke specific signaling pathways which might regulate cellular phenotype and function [38–41]. Ranucci and Moghe [29] studied the adhesion and motility behavior of HepG2 cells on microtextured copolymer substrates. Immunofluorescent labeling of vinculin revealed a streaked pattern throughout the ventral surface for the cells cultured on the textured surface. In contrast, vinculin-rich regions were not detected in cells cultured on the untextured surface. As such, vinculin was used as an indicator of cytoskeletonal reorganization on substrate [29]. For the present investigations, the presence of focal adhesions and cytoskeletonal reorganization were also assessed through expression of vinculin.

The micrometer-size pits on the substrates could have another topographical effect on the cultured cells. Previous research showed that migration of corneal epithelial cells was not inhibited on polycarbonate membranes with pore diameters even as large as 2.3-μm, although the migration was reduced on membranes having pore sizes larger than 0.9 μm [22]. Inhibition of membrane protrusion at the pores could be a possible explanation for the reduced migration. Under such circumstances, cells would be largely contained by the track-etch pits and the cell membrane edges would tend to be in contact with the track-etch pits. This possibility was assessed by correlation analyses between the positions of track-etch pits and cells on captured images.

In brief, the main objective of the present work was to explore the feasibility of using pits created on the surface of a polymer by alpha-particle irradiation and subsequent chemical etching to study the substrate topographical effects on cell behaviors. The pits were purposely not etched-through so no extra and sophisticated steps were required for blind-ending.

2. Methodology

2.1. PADC films, treatments and characterization

In the present work, polyallyldiglycol carbonate (PADC) films (commercially available as CR-39 detectors) were used as the cell substrates. CR-39 detectors are one of the most commonly used solid-state nuclear track detectors (SSNTDs). A recent review on SSNTDs has been given in [27]. In the present work, CR-39 SSNTDs with a thickness of 1000 μm were purchased from Page Mouldings (Pershore) Limited, Worcestershire. A number of PADC films with a size of 2×2 cm^2 were prepared and subjected to different treatments before cell cultivation. These include raw and unetched films, etched blank (unirradiated) films and etched irradiated films. Irradiations were made with 3 MeV alpha particles from a planar ^{241}Am source (main alpha energy = 5.49 MeV under vacuum) for durations of 3 and 6 h. For an irradiation time of 3 h, the average track density is about 4.15×10^5 tracks cm^{-2}. The final alpha energies incident on the films were controlled by the source to film distances in normal air. The relationship between the alpha energy and the air distance traveled by an alpha particle with initial energy of 5.49 MeV from ^{241}Am was obtained by measuring the energies for alpha particles passing through different distances in normal air using alpha spectroscopy systems (ORTEC Model 5030) with passivated implanted planar silicon (PIPS) detectors of areas of 300 mm^2. Etching was performed first for 3 h in 6.25 N aqueous NaOH at 70 °C (which corresponded to a bulk etch rate of 1.2 μm/h [42]) and then for 5 min in 1 N NaOH/ethanol at 40 °C (which corresponded to a bulk etch rate of ~9.5 μm/h [43]). These etching conditions produced superficial etch pits with sizes much smaller than the dimensions of the HeLa cells. The films were etched in NaOH/ethanol in the end since NaOH/ethanol-etched PADC films were more biocompatible than the NaOH/H_2O-etched PADC films [44].

To characterize the surface topography of the irradiated and etched PADC films, the size of the track-etch pits were determined from their lateral images after polishing the edge of the films [45]. For a comparison, the opening diameters of alpha-particle track-etch pits in PADC films formed by etching in NaOH/H_2O alone were calculated using the computer program called TRACK_TEST [46] (also available on the webpage: http://www.cityu.edu.hk/ap/nru/test.htm). It is remarked here that the opening

diameters can no longer be simulated using TRACK_TEST after a further etching in NaOH/ethanol for 5 min, since the V function (ratio between the track etch rate and the bulk etch rate) of PADC in NaOH/ethanol, which is required by the TRACK_TEST program for computation, is unknown.

2.2. Cell culture

HeLa cervix cancer cells were cultured on the $2 \times 2\ cm^2$ PADC films subjected to different treatments as described in Section 2.1. Before cell culture, the PADC films were sterilized by submerging in 75% (v/v) ethyl alcohol for 2 h and then in absolute alcohol. These films were then used for culturing National Institutes of Health HeLa cervix cancer cells obtained from the American Type Culture Collection. The cell line was maintained as exponentially growing monolayers at low-passage numbers in Dulbecco's modified eagle medium (D-MEM) supplemented with 10% fetal bovine serum, 1% (v/v) penicillin/streptomycin. The cells were cultured at 37 °C in humidified atmosphere containing 5% CO_2. Subcultivation was performed every 3–4 d. Penicillin/streptomycin was produced by Gibco (Karlsrube, Germany). The cells were trypsinized with 0.5/0.2% (v/v) trypsin/EDTA (ethylenediamine-tetra-acetic acid; Gibco), adjusted to desired concentrations and plated out on the PADC films placed inside a 90 mm diameter Petri dish. During the plate out, each Petri dish contained PADC films subjected to all different treatments as described in Section 2.1.

For the cell area and immunohistochemical localization studies, the concentrations were adjusted to 0.5×10^4 and 10^4 cells ml^{-1}, respectively (with a total volume of 25 ml). For analyzing the cell number, vinculin expression (SDS-PAGE) as well as the correlation between the positions of cells and track-etch pits, the concentrations were adjusted to 5×10^4 cells m^{-1} (with a total volume of 25 ml). All cells were allowed to plate out on the PADC films for 3 d.

2.3. Immunohistochemical localization studies

Immunohistochemical localization studies were carried out to visualize the expression of vinculin. Briefly, the cells cultured on PADC films subjected to different treatments as described in Section 2.1 were fixed with 4% formaldehyde and permeabilized with 0.1% Triton X-100. Nonspecific binding sites were blocked with 3% bovine serum albumin and 1% normal goat serum in PBS (Gibco) for 1 h at room temperature. Subsequently, the samples were incubated for 1 h with a mouse monoclonal antibody (mAB) to human vinculin (Chemicon International, CA; diluted 1:20 in blocking solution), washed four times (15 min each) with PBS, and incubated with Cy3-conjugated AffiniPure Goat Anti-Rabbit IgG (H+L) (Jackson ImmunoResearch; diluted 1:200 in blocking solution). After a 1-h incubation period, the secondary antibody was removed and the samples were washed in PBS overnight at 4 °C. The samples were then mounted in a fluorescent mounting medium (Dako) before imaging with a laser-scanning confocal microscope (Carl Zeiss Laser Scanning Microscope) at 800× magnification.

2.4. Vinculin expression studies

SDS-PAGE was performed as described [47]. The blocked PVDF membrane was incubated with vinculin antibody (Chemicon International, CA; diluted 1:200 in blocking solution (2% BSA, 0.1% Tween-20 (v/v) and 1xPBS (0.1 M Na_2HPO_4, 0.1 M NaH_2PO_4, 0.5 M NaCl)) overnight at 4 °C, washed with 0.1% TPBS (0.1% Tween-20 (v/v) and 1×PBS) three times for 15 min each at room temperature and incubated with the horseradish peroxidase conjugated goat anti-rabbit IgG (Dako) at 1:5000 dilution at room temperature for 1 h. Then, the membrane was washed three times with 0.1% TPBS for 15 min each and bands were detected by ECL kit (Amersham). Density of each band was quantified by ImageJ software (http://rsb.info.nih.gov/ij/). Data are presented as fold changes. The Coomassie-Blue stained gel image was served as a protein loading control [48–51].

2.5. Cell proliferation studies

In order to count the cell number on different CR-39 SSNTDs, the attached cells on the various films were released by digestion with trypsin–ethylenediaminetetraacetic acid (Invitrogen) and counted using a hemocytoeter (Marienfeld, Germany).

2.6. Correlation between the positions of track-etch pits and cells

In order to study the correlation between the positions of track-etch pits and cells, images of the etched PADC films which had been irradiated with alpha particles for 3 or 6 h together with the cultured HeLa cells were captured under the optical microscope with a magnification of 200× in the transmission mode. The track-etch pits on each PADC film was categorized as (1) those in contact with cell membrane edges, (2) those covered by the cell core bodies, (3) those not in contact with the cells and (4) unclassified, where the pits were close to cell membrane edges, but decisions on the contacts could not be made without ambiguity.

2.7. Cell area and perimeter measurement and statistics

The cell areas and perimeters were measured by the ImageJ software. Student's t-test (for two samples, assuming unequal variances) was used to compare statistical significance of test materials against the control by SigmaPlot (Systat Software Inc.). Results with $p < 0.05$ were considered statistically significant.

3. Results

3.1. Topography of alpha-particle irradiated and chemically etched PADC films

For the irradiated and etched PADC films, the average opening diameter and depth of the track-etch pits after etching in $NaOH/H_2O$ with the additional etching by NaOH/ethanol for 5 min determined from their lateral images after polishing the edge of the film [45] were 4.8 ± 0.1 and 6.6 ± 0.3 μm, respectively. Fig. 1 shows the lateral view of a conical track revealed under the optical microscope operated in the transmission mode after polishing the edge of the film. Without the additional etching by NaOH/ethanol, the opening diameter and depth calculated by the computer program TRACK_TEST [46] were 4.6 and 6.2 μm, respectively.

3.2. Immunohistochemical localization studies

Fig. 2(A) shows the expression of vinculin on HeLa cells cultured on the PADC films subjected to different treatments. In Fig. 2(A), the images from confocal microscope, the transmission mode optical images as well as their superpositions are shown. From Fig. 2(A), we observe overall increases in vinculin expression for HeLa cells cultured on PADC films with track-etch pits. On the contrary, vinculin-rich regions were not revealed in cells cultured on the raw (unetched) as well as the blank (etched) PADC films. Similar observations were obtained for HepG2 cells cultured on untextured and microtextured copolymer substrates [29].

3.3. Western blotting study

Fig. 2(B) illustrates the expression of vinculin. Here, representative images from western blotting are shown, where the size of vinculin protein is about 117 kDa. The respective bands which represent the expression of vinculin from proteins sampled from HeLa cells cultured on PADC films with track-etch pits were stronger than those for cells cultured on the raw (unetched) as well as on the blank (etched) PADC films. The results for cells cultured on track-etch pits and those cultured on the raw detectors were found to be statistically significant ($p < 0.05$).

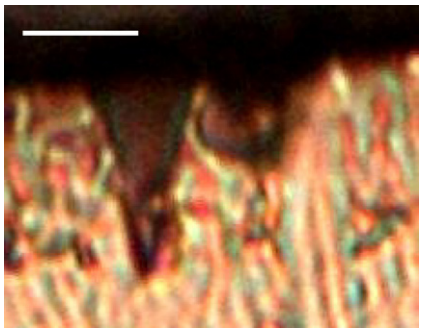

Fig. 1. The lateral view of a conical pit generated from an alpha particle with incident energy of 3 MeV (etched for 3 h in 6.25 N aqueous NaOH at 70 °C and then for 5 min in 1 N NaOH/ethanol at 40 °C) revealed under the optical microscope operated in the transmission mode after polishing the edge of the film. Bar = 5 μm.

3.4. Effects of substrate pits on cell growth, area and circularity

The proliferation rate of HeLa cells was indicated by the number of cells measured after the cells had been cultured on substrates for 3 d (Fig. 6). Cells growing on 3-h etched PADC films were found to be only one-fourth those growing on raw films. On the other hand, etched films with track-etch pits were found to have significantly increased the number of cells, by comparing with the number of cells growing on the 3-h etched blank films ($p < 0.05$).

The area of cells growing on the etched blank films or track-etch pits on films were found to be significantly smaller than the area of cells growing on raw films ($p < 0.05$) (Fig. 7).

The circularity of cells, calculated using the definition of $4\pi \times (\text{area}/\text{perimeter}^2)$ from Lim et al. [16], indicates the elongated polygonal-shaped spreading of cells. According to this definition, the circularity of cells would increase when the polygonal-shaped spreading of the cells was reduced. When cell spreading was induced on etched blank PADC films (Fig. 2(A)), circularity of cells was lower (Fig. 8). On the other hand, track-etch pits on films suppressed the polygonal-shaped spreading of cells. The circularity of cells growing on PADC films irradiated by 3 MeV alpha particles for 6 h and then etched was similar to cells growing on raw films. These results suggested that cell membrane edges in contact with the pits suppressed further polygonal-shaped spreading of the cells.

Cells growing on etched blank PADC films had smaller cell areas but with more elongated polygonal-shaped spreading (lower circularity) when compared to cells growing on raw films. This suggested that etching alone reduced cell growth (proliferation) and area but induced polygonal-shaped spreading.

Cells growing on track-etch pits on PADC films also had smaller cell areas than cells growing on raw films, but were more in number than cells growing on etched blank films. When irradiation was prolonged from 3 h to 6 h, the projections measured on the cells growing on track-etch pits on films were reduced and, in other words, the circularity of the cells increased. This suggested that pits alone on films induced cell growth and circularity but did not increase the cell area.

Taken together the observations from cell growth (proliferation), area and circularity, track-etch pits on PADC films reduced cell proliferation, elongated polygonal-shaped spreading and cell area.

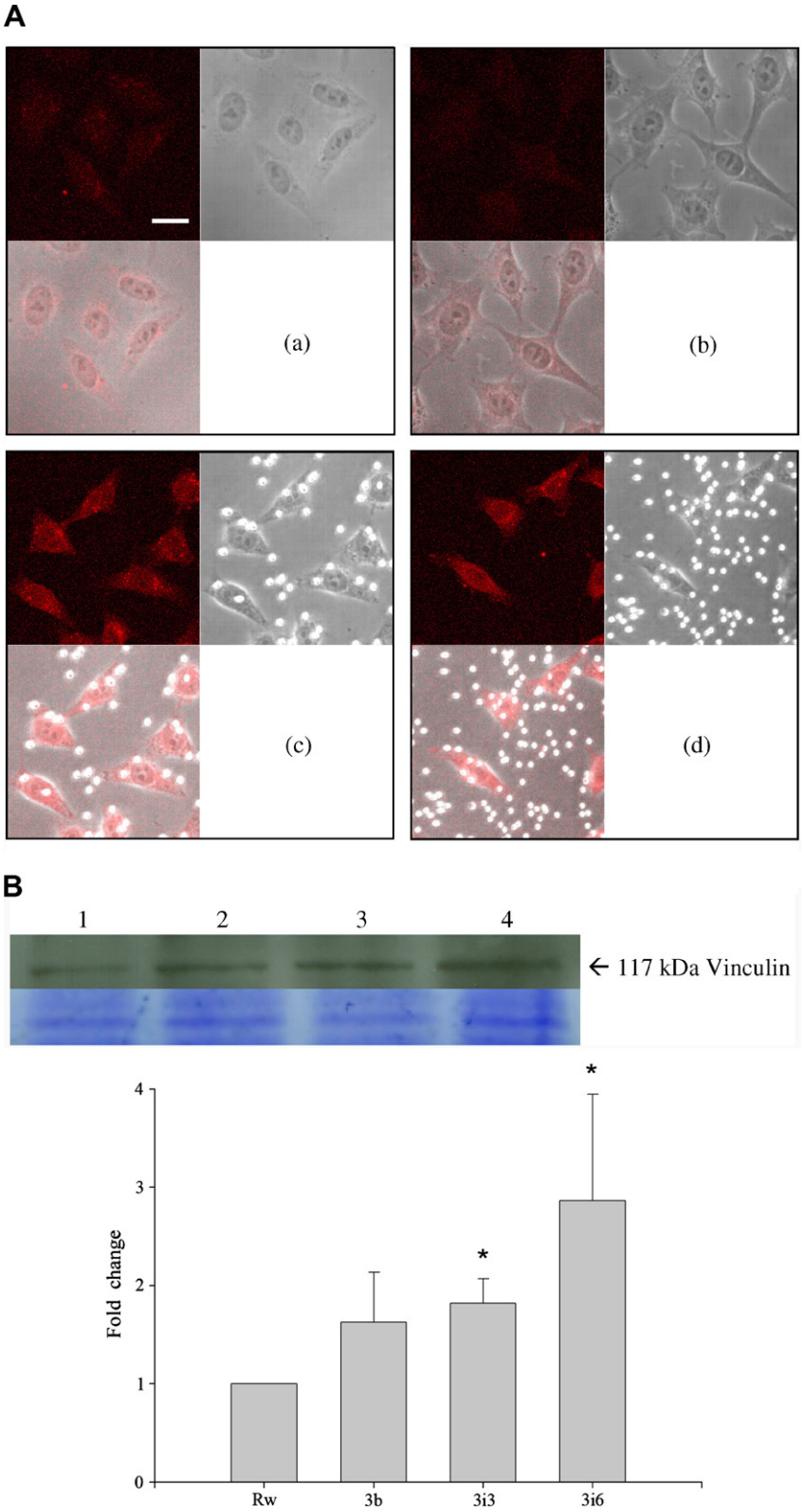

Fig. 2. (A) Representative images showing the spatial expression of vinculin on HeLa cells on (a) raw and unetched PADC film; (b) etched blank PADC film; (c) PADC film irradiated by 3 MeV alpha particles for 3 h and etched; (d) PADC film irradiated by 3 MeV alpha particles for 6 h and etched. For (b), (c) and (d), etching was performed for 3 h in 6.25 N aqueous NaOH at 70 °C and then for 5 min in 1 N NaOH/ethanol at 40 °C. Bar = 20 μm; $n = 3$; (a) to (d) are at identical magnification. For (a) to (d), *upper left:* images from confocal microscope; *upper right:* transmission mode optical images; *lower left:* superposition of the upper left and upper right images. (B) Vinculin detected by immunoblot presented as fold changes. Upper image lanes: 1, Rw (blank and unetched film); 2, 3 b (3 h etched blank film); 3, 3i3 (etched film with 3 h irradiation); 4, 3i6 (etched film with 6 h irradiation). Right margin arrow, molecular weight standard. Below, identically loaded Coomassie-stained gel (loading controls). 3i3 and 3i6 showed statistically significant increases compared with raw ($^{*}p < 0.05$, mean + SD, $n = 3$).

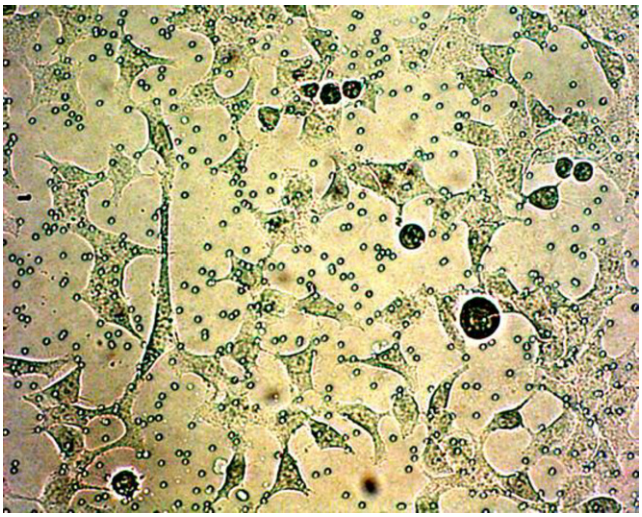

Fig. 3. An image (200× in the transmission mode) showing the superposition of HeLa cells cultured for 3 d and track-etch pits generated from irradiation of 3 MeV alpha particles for 3 h, etched for 3 h in 6.25 N aqueous NaOH at 70 °C and then for 5 min in 1 N NaOH/ethanol at 40 °C.

3.5. Correlation between positions of track-etch pits and cells

Images of etched PADC films which had been irradiated with alpha particles for 3 or 6 h together with the cultured HeLa cells were captured under the optical microscope with a magnification of 200× in the transmission mode. Fig. 3 shows a representative image corresponding to 3-h alpha-particle irradiation.

The number of track-etch pits in contact with cell membrane edges (E) and those covered by the cell core bodies (B), as well as those not in contact with the cells (N) were counted. There were some unclassified cases where the pits were close to cell membrane edges, but decisions on actual contacts could not be made without ambiguity, and the corresponding number was recorded as (U). The total number of counted pits was $T = E + B + N + U$. A total of 3 images corresponding to 3-h alpha-particle irradiation, with the superposition of HeLa cells and the track-etch pits, were analyzed for these numbers. The results are shown in Table 1.

In order to have a better understanding of the numbers in Table 1(a) and (b), we also performed a computer simulation for the case where the track-etch pits were randomly distributed. The average total number of track-etch pits was calculated from the total number of track-etch pits in the three samples, which was $(701 + 635 + 562)/3 = 633$. The average total track-etch pit density was determined as 4.15×10^5 tracks cm^{-2}. The 633 track-etch pits were randomly distributed in the area of the image. The actual images of the cells were then superimposed onto the images of these randomly distributed track-etch pits. Fig. 4 is the superposition of images of the randomly distributed track-etch pits and the images of HeLa cells shown in Fig. 3. The numbers E, B, N, U and T were again counted

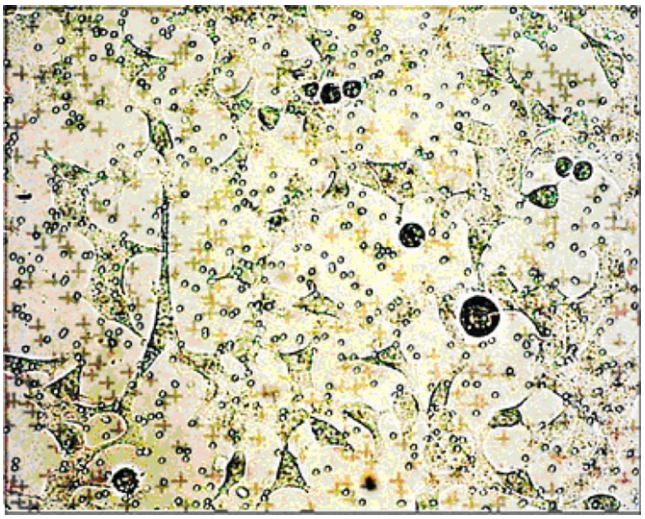

Fig. 4. Superposition of positions of randomly distributed track-etch pits (pluses) and the image shown in Fig. 3.

Table 1
Panel (a): the number of track-etch pits in contact with cell membrane edges (E), covered by the cell core bodies (B), not in contact with the cells (N), unclassified (U) and the total number ($T = E + B + N + U$) obtained for the images of the three samples corresponding to 3-h alpha-particle irradiation; panel (b): the numbers in (a) converted to ratios to T

	Sample 1	Sample 2	Sample 3
Panel (a)			
E	323	267	244
B	67	63	55
N	133	212	212
U	178	93	51
T	701	635	562
Panel (b)			
E/T	0.461	0.420	0.434
B/T	0.096	0.099	0.098
N/T	0.190	0.334	0.377
U/T	0.254	0.146	0.091

Table 2
Panel (a): the number of computer-simulated track-etch pits in contact with cell membrane edges (E), covered by the cell core bodies (B), not in contact with the cells (N), unclassified (U) and the total number ($T = E + B + N + U$) obtained for the images of the three samples corresponding to 3-h alpha-particle irradiation; panel (b): the numbers in (a) converted to ratios to T

	Sample 1	Sample 2	Sample 3
Panel (a)			
E	72	95	130
B	111	152	210
N	272	288	178
U	178	88	115
T	633	633	633
Panel (b)			
E/T	0.114	0.150	0.205
B/T	0.175	0.240	0.332
N/T	0.430	0.455	0.281
U/T	0.281	0.139	0.182

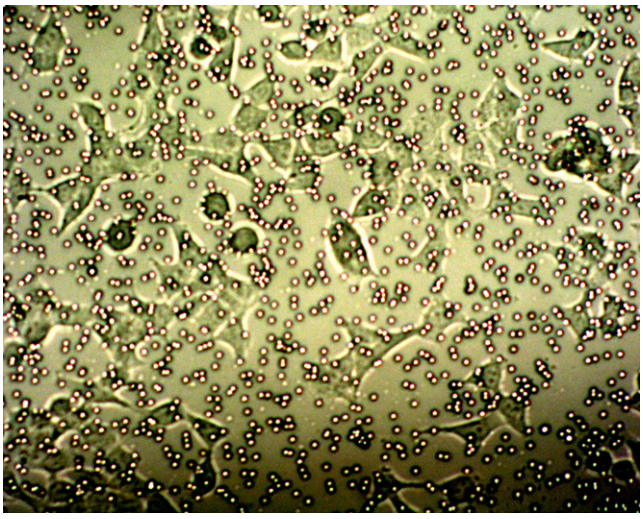

Fig. 5. An image (200× in the transmission mode) showing the superposition of HeLa cells cultured for 3 d and track-etch pits generated from irradiation of 3 MeV alpha particles for 6 h, etched for 3 h in 6.25 N aqueous NaOH at 70 °C and then for 5 min in 1 N NaOH/ethanol at 40 °C.

as described above. The results are shown in Table 2. From Table 1b and 2b, we observed that the percentages of track-etch pits in contact with cell membrane edges, viz. E/T, in the real cases were much larger than those in the simulated cases.

Fig. 5 shows one of the images corresponding to 6-h alpha-particle irradiation. A higher etch-pit density is apparent. The numbers E, B, N, U and T were again counted as described above, and the results are shown in Table 3. By comparing Table 1b and 3b, we observed that the E/T percentages were commensurate for 3- and 6-h alpha-particle irradiation.

4. Discussion

This study explored the feasibility of using track-etch pits on the surface of a polymer to study the substrate topographical effects on epithelial cell behaviors. The effects were studied in terms of (1) focal adhesions and cytoskeletonal reorganization through examination of vinculin expression; and (2) contact of cell membrane edges with the pits. Our results demonstrated that substrate track-etch pits were an important determinant of epithelial cell behaviors.

Vinculin is a cell adhesion and membrane protrusion protein coupled with integrins, paxillin, talin and actin filaments [52–56]. It is part of the focal adhesion complex linking F-actin filaments to cell membrane sites within 15 nm of the underlying substrate [47,57], and plays an essential role in cell modeling, adhesion structure modulation and motility [47,58]. As such, vinculin is used as an

Table 3
Panel (a): the number of track-etch pits in contact with cell membrane edges (E), covered by the cell core bodies (B), not in contact with the cells (N), unclassified (U) and the total number ($T = E + B + N + U$) obtained for the images of the three samples corresponding to 6-h alpha-particle irradiation; panel (b): the numbers in (a) converted to ratios to T

	Sample 1	Sample 2	Sample 3
Panel (a)			
E	569	644	620
B	83	89	176
N	652	389	324
U	102	71	53
T	1406	1193	1173
Panel (b)			
E/T	0.405	0.540	0.529
B/T	0.059	0.075	0.150
N/T	0.464	0.326	0.276
U/T	0.073	0.060	0.045

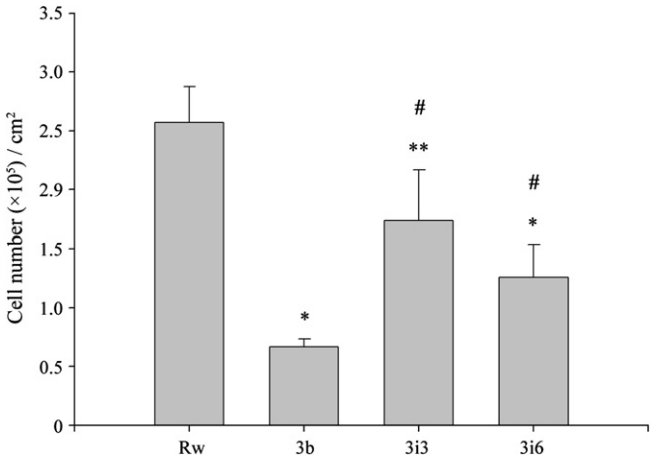

Fig. 6. Number of HeLa cells on different treated PADC films. That for Rw is significantly different from those for 3b and 3i6 ($^{*}p < 0.05$, mean + SD, $n = 3$) as well as 3i3 ($^{**}p < 0.06$, mean + SD, $n = 3$) and that for 3i3, 3i6 is significantly different from 3b ($\#p < 0.05$, mean + SD, $n = 3$). For the sample codes, the readers are referred to the caption for Fig. 2.

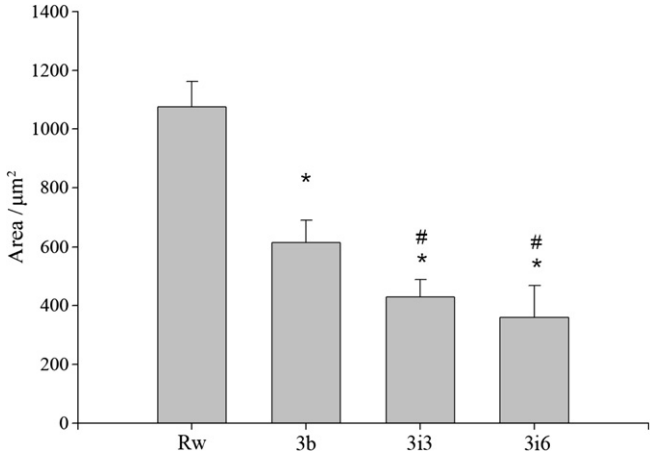

Fig. 7. Area of cells. The areas of cells cultured on the 3b, 3i3 and 3i6 samples were significantly smaller than that for Rw ($^{*}p < 0.05$, mean + SD, $n = 3$), whereas the areas of cells cultured on the 3i3 and 3i6 samples were also significantly smaller than that for 3b ($\#p < 0.05$). For the sample codes, the readers are referred to the caption for Fig. 2.

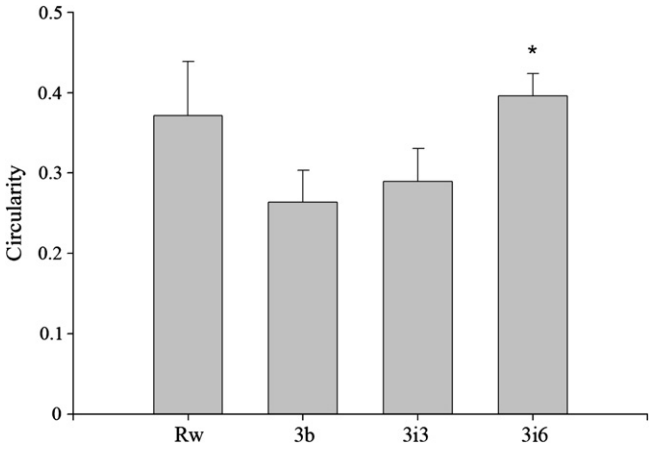

Fig. 8. Circularity of cells. Circularity for cells cultured on the 3i6 sample was significantly larger than those cultured on the 3b and 3i3 samples ($^{*}p < 0.05$, mean + SD, $n = 3$). For the sample codes, the readers are referred to the caption for Fig. 2.

indicator of cytoskeletonal reorganization on substrate [29] and localization of vinculin is often used to demonstrate the presence of focal adhesions [34–36].

Focal adhesion and motility of cells on their ECM involved a series of molecular signaling mechanisms. Potential signaling mechanisms upon cell contact with a matrix were suggested [52–55,59,60]. Numerous regulatory molecules including RNA and DNA synthesis, associated with numerous enzymes and substrates mediating different signaling pathways scaffold the cytoskeleton of the cell [59]. In particular, integrin receptors on the cell membrane recruit the Arp2/3 complex which interacts with focal adhesion proteins such as vinculin, talin and paxillin coupling the actin polymerization machinery and activates focal adhesion kinase as well as other signaling cascades. Ranucci and Moghe [29] suggested that the presence of micropores on the substrate might locally effect the clustering of integrin receptors. These integrin clustering events can lead to signal transduction [61], including activation of focal adhesion kinase, which is a prerequisite for cell migration [62].

Our immunofluorescent results revealed that there is a general increase of vinculin expression of HeLa cells cultured on PADC films with track-etch pits, but not in cells cultured on the raw (unetched) as well as the blank (etched) PADC films. In other words, vinculin expression was induced by the topography of track-etch pits, while etching of the substrate alone (without alpha-particle irradiation) did not cause up-regulation of vinculin protein expression. Results were confirmed with western blotting. The results were in general consistent with those of Ranucci and Moghe [29] who studied the adhesion and motility behavior of HepG2 cells on microtextured copolymer substrates. In the absence of surface-adsorbed collagen ligand, vinculin localized throughout the ventral surface of the cells in contact with the textured substrate but was not detected at all on cells in contact with the untextured surface [29]. The cell adhesive behavior was explained in terms of changes in the intracellular organization of the cytoskeleton-associated protein vinculin and the extent and strength of cell adhesion to the substrate [29]. They expected their vinculin-based results to be a result of cytoskeletal reorganization on microtextured copolymer substrates, because previous studies [63] showed that actin aggregation behavior at textural discontinuities was correlated with vinculin dynamics during cell orientation on microgrooved substrates. Another previous study with primary hepatocytes [9] also showed the presence along the ventral cell surface of F-actin rings, whose location and size corresponded to the substrate micropores. These findings were also in general agreement with the related study by Evans et al. [24] who evaluated the ultrastructure of the corneal epithelial tissue – polycarbonate membrane interface for the formation of the basal lamina component of the basement membrane and the electron-dense hemidesmosomal plaque component of the adhesion complexes associated with the cytoplasmic side of the basal cell membrane. Assembly of adhesive structures at the tissue–polymer interface was facilitated with the introduction of pores into a solid polycarbonate surface, while structures resembling either basement membrane or hemidesmosomal plaque at the tissue–polymer interface were not formed by cells cultured on the nonporous polycarbonate polymer surface [24]. The observations were also consistent with those for MDCK cells grown on solid plastic surfaces [64,65]. In summary, the results of vinculin suggested that the substrate topography changed the focal adhesions and cytoskeletonal reorganization of cells.

For the HeLa cells cultured on PADC films with track-etch pits, besides vinculin expression, changes of cell proliferation, cell area and circularity were also observed. A closer look at the cells cultured on PADC films with track-etch pits revealed that the cells were largely contained by the track-etch pits. In other words, the cell membrane edges tended to be in contact with the pits. By comparing the correlation between the positions of HeLa epithelial cells and the track-etch pits on PADC films, and that between the positions of cells and computer-simulated pits, the tendency for membrane edges of HeLa epithelial cells to be in contact with the track-etch pits could indeed be recognized. A higher etch-pit density also resulted in a higher number of etch pits in contact with the cell membrane edges, but the percentage of these etch pits to the total number of etch pits remained more or less the same. Inhibition of membrane protrusion at the pores could explain this phenomenon, as well as the reduced migration of corneal epithelial cells on polycarbonate membranes having pore sizes larger than 0.9 μm [22]. A previous study on movement of 3T3 fibroblasts on polyacrylamide sheets with discontinuities in rigidity showed that, when the cells approached the boundary from the stiff side, protrusion stopped at the leading edge and then continued laterally along the boundary, causing the cell to change shape and orientation [66].

In this study, we presented a simple and convenient way of introducing micrometer-size pits on the surface of a polymer (PADC) substrate by alpha-particle irradiation and subsequent chemical etching. These pits are useful for examining the topographical effects on cell behaviors. In fact, this method has a whole range of flexibilities in generating pits with different characteristics. For example, the pit density can be simply controlled by the alpha-particle irradiation time while the pit-opening diameter can be controlled by the etching duration. The sizes of the pits together with the amount of polymer surface between pits are equivalent to the pitch used in contact guidance experiments with substrate surfaces micropatterned with grooves [24]. The track-etch pits employed in the current study were conical, but other pit profiles such as spherical, or conical at the top and spherical at the bottom are also possible by controlling the alpha-particle incident energy and the etching duration. Profiles can be conveniently designed with the help of the TRACK_TEST computer program [46]. Pits making different angles with the substrate surface can be generated by varying the incident angles of the alpha particles. In these cases, the opening will become elliptical or egg-shaped depending on the etching duration. Combinations of pits described above can also be conveniently introduced to the substrate surface.

5. Conclusions

Topography affects cell behavior as demonstrated by the increase in expression of the focal adhesion protein vinculin in HeLa cells cultured on PADC films with track-etch pits, but not in cells cultured on the raw or chemically etched blank PADC films. Topography also affects cell proliferation, area and circularity. HeLa cells cultured on PADC films with track-etch pits also showed changes in cell proliferation, cell area and cell circularity, and were largely contained by the track-etch pits. This could be explained by inhibition of membrane protrusion at the pores. Our results demonstrated that substrate track-etch pits were an important determinant of epithelial cell behaviors.

References

[1] H.L. Wald, G. Sarakinos, M.D. Lyman, A.G. Mikos, J.P. Vacanti, R. Langer, Biomaterials 14 (1993) 270.
[2] E. Wintermantel, J. Mayer, J. Blum, K.-L. Eckert, P. Lüscher, M. Mathey, Biomaterials 17 (1996) 83.
[3] D. Mooney, K. Sano, P.M. Kaufmann, K. Majahod, B. Schloo, J. Vacanti, R. Langer, J. Biomed. Mater. Res. 37 (1996) 413.
[4] U. Kneser, P.M. Kaufmann, H.C. Fiegel, J.M. Pollok, D. Kluth, H. Herbst, X. Rogiers, J. Biomed. Mater. Res. 47 (1999) 494.
[5] M. Lampin, R. Warocquier-Clerout, C. Legris, M. Degrange, M.F. Sigot-Luizard, J. Biomed. Mater. Res. 36 (1997) 99.
[6] J.S. Burmeister, J.D. Vrany, W.M. Reichert, G.A. Truskey, J. Biomed. Mater. Res. 30 (1996) 13.
[7] E. Eisenbarth, J. Meyle, W. Nachtigall, J. Breme, Biomaterials 17 (1996) 1399.
[8] A. Curtis, C. Wilkinson, Biomaterials 18 (1997) 1573.
[9] C.S. Ranucci, P.V. Moghe, Tissue Eng. 5 (1999) 407.
[10] N. Krasteva, B. Seifert, W. Albrecht, T. Weigel, M. Schossig, G. Altankov, T. Groth, Biomaterials 25 (2004) 2467.
[11] S.J. Lee, J.S. Choi, K.S. Park, G. Khang, Y.M. Lee, H.B. Lee, Biomaterials 25 (2004) 4699.
[12] C.C. Berry, G. Campbell, A. Spadiccino, M. Robertson, A.S.G. Adam, S.G. Curtis, Biomaterials 25 (2004) 5781.
[13] Y. Wan, Y. Wang, Z. Liu, X. Qu, B. Han, J. Bei, S. Wang, Biomaterials 26 (2005) 4453.
[14] M.J. Dalby, D. McCloy, M. Robertson, C.D.W. Wilkinson, R.O.C. Oreffo, Biomaterials 27 (2006) 1306.
[15] H. Zimmermanna, F. Wählischb, C. Baierb, M. Westhoffb, R. Reussb, D. Zimmermannc, M. Behringerb, F. Ehrharta, A. Katsen-Globaa, C. Giesed, U. Marxd, V.L. Sukhorukovb, J.A. Vásqueze, P. Jakobf, S.G. Shirleya, U. Zimmermannb, Biomaterials 28 (2007) 1327.
[16] J.Y. Lim, A.D. Dreiss, Z. Zhou, J.C. Hansen, C.A. Siedlecki, R.W. Hengstebeck, J. Cheng, N. Winograd, H.J. Donahue, Biomaterials 28 (2007) 1787.
[17] D.W. Hamilton, D.M. Brunette, Biomaterials 28 (2007) 1806.
[18] M.Y.H. Chin, A. Sandham, J. de Vries, H.C. van der Mei, H.J. Busscher, Biomaterials 28 (2007) 2032.
[19] D.W. Hamilton, B. Chehroudi, D.M. Brunette, Biomaterials 28 (2007) 2281.
[20] C.A. Squier, P. Collins, J. Periodontal Res. 16 (1981) 434.
[21] S. Takeuchi, Develop. Biol. 51 (1976) 49.
[22] J.H. Fitton, B.A. Dalton, G. Beumer, G. Johnson, H.J. Griesser, J.G. Steele, J. Biomed. Mater. Res. 42 (1998) 245.
[23] B.A. Dalton, M.D.M. Evans, G.A. McFarland, J.G. Steele, J. Biomed. Mater. Res. 45 (1999) 384.
[24] M.D.M. Evans, B.A. Dalton, J.G. Steele, J. Biomed. Mater. Res. 46 (1999) 485.
[25] B.A. Dalton, G.A. McFarland, J.G. Steele, J. Biomed. Mater. Res. 56 (2001) 83.
[26] M.D.M. Evans, S. Taylor, B.A. Dalton, D. Lohmann, J. Biomed. Mater. Res. 64A (2003) 357.
[27] D. Nikezic, K.N. Yu, Mater. Sci. Eng. R 46 (2004) 51.
[28] A.K. Harris Jr., J. Biotechnol. Eng. 106 (1984) 19.
[29] C.S. Ranucci, P.V. Moghe, J. Biomed. Mater. Res. 54 (2001) 149.
[30] B. Baharloo, M. Textor, D.M. Brunette, J. Biomed. Mater. Res. 74A (2005) 12.
[31] D.C. Anderson, T.A. Springer, Ann. Rev. Med. 38 (1987) 175.
[32] C.A. Buck, A.F. Horwitz, Ann. Rev. Cell. Biol. 3 (1987) 179.
[33] R.O. Hynes, Cell 48 (1987) 549.
[34] B. Geiger, Cell 18 (1979) 193.
[35] B. Geiger, E. Schmid, W.W. Franke, Differentiation 23 (1983) 189.
[36] R.G. Richards, M. Stiffanic, G.R.H. Owen, M. Riehle, I.P. Gwynn, A.S.G. Curtis, Cell Biol. Int. 25 (2001) 1237.
[37] T.G. Van Kooten, A.F. Von Recum, Tissue Eng. 5 (1999) 223.
[38] J. Meyle, K. Gultig, J. Wolburg, A.F. Von Recum, J. Biomed. Mater. Res. 27 (1993) 1553.
[39] L. Chou, J.D. Firth, V.J. Uitto, D.M. Brunette, J. Cell Sci. 108 (1995) 1563.
[40] Z. Schwartz, J.Y. Martin, D.D. Dean, J. Simpson, D.L. Cochran, B.D. Boyan, J. Biomed. Mater. Res. 30 (1996) 145.
[41] K. Kieswetter, Z. Schwartz, T.W. Hummert, D.L. Cochran, J. Simpson, D.D. Dean, B.D. Boyan, J. Biomed. Mater. Res. 32 (1996) 55.
[42] J.P.Y. Ho, C.W.Y. Yip, D. Nikezic, K.N. Yu, Radiat. Meas. 36 (2003) 141.
[43] K.F. Chan, B.M.F. Lau, D. Nikezic, A.K.W. Tse, W.F. Fong, K.N. Yu, Nucl. Instr. and Meth. B 263 (2007) 290.
[44] W.Y. Li, K.F. Chan, A.K.W. Tse, W.F. Fong, K.N. Yu, Nucl. Instr. and Meth. B 248 (2006) 319.
[45] B. Dörschel, D. Fülle, H. Hartmann, D. Hermsdorf, K. Kadner, Ch. Radlach, Radiat. Prot. Dosim. 69 (1997) 267.
[46] D. Nikezic, K.N. Yu, Comput. Phys. Commun. 174 (2006) 160.
[47] W.H. Goldmann, D.E. Ingber, Biochem. Biophys. Res. Commun. 290 (2002) 749.

[48] A.S. Pearson, F.R. Spitz, S.G. Swisher, M. Kataoka, M.G. Sarkiss, R.E. Meyn, T.J. McDonnell, R.J. Cristiano, J.A. Roth, Clin. Cancer Res. 6 (2000) 887.
[49] O. Casanovas, M. Jaumot, A.-B. Paules, N. Agell, O. Bachs, Oncogene 23 (2004) 7537.
[50] G. Lomberk, D. Bensi, M.E. Fernandez-Zapico, R. Urrutia, Nat. Cell Biol. 8 (2006) 407.
[51] D.L. Woodhall, I.J. Groves, M.B. Reeves, G. Wilkinson, J.H. Sinclair, J. Biol. Chem. 281 (2006) 37652.
[52] K.A. DeMali, K. Burridge, J. Cell Sci. 116 (2003) 2389.
[53] D.E. Discher, P. Janmey, Y.L. Wang, Science 310 (2005) 1139.
[54] K. Hu, L. Ji, K.T. Applegate, G. Danuser, C.M. Waterman-Storer, Science 315 (2007) 111.
[55] A. Katsumi, A.O. Orr, E. Tzima, M.A. Schwartz, J. Biol. Chem. 279 (2004) 12001.
[56] D. Motlagh, S.E. Senyo, T.A. Desai, B. Russell, Biomaterials 24 (2003) 2463.
[57] G. Schneider, K. Burridge, Exp. Cell Res. 214 (1994) 264.
[58] R.M. Ezzell, W.H. Goldmann, N. Wang, N. Parasharama, D.E. Ingber, Exp. Cell Res. 231 (1997) 14.
[59] D.E. Ingber, I.I. Tensegrity, J. Cell Sci. 116 (2003) 1397.
[60] B. Katz, E. Zamir, A. Bershadsky, Z. Kam, K.M. Yamada, B. Geiger, Mol. Biol. Cell 11 (2000) 1047.
[61] L.J. Kornberg, H.S. Earp, C.E. Turner, C. Prockop, R. Juliano, Proc. Natl. Acad. Sci. USA 88 (1991) 8392.
[62] D.J. Sieg, C.R. Hauck, D.D. Schlaepfer, J. Cell Sci. 112 (1999) 2677.
[63] B. Wojciak-Stothard, A.S.G. Curtis, W. Monaghan, M. McGrath, I. Sommer, C.D.W. Wilkinson, Cell Motil. Cytoskel. 31 (1995) 147.
[64] J.R. Cook, B.E. Crute, L.M. Patrone, J. Gabriels, M.E. Lane, R.G. Van Buskirk, In Vitro Cell Dev. Biol. 25 (1989) 914.
[65] W. Karst, H.J. Merker, Cell Different. 22 (1988) 211.
[66] C. Lo, H. Wang, M. Dembo, Y.-l. Wang, Biophys. J. 79 (2000) 144.